Supporting Information for

Real-time chemical characterization of primary and aged biomass burning aerosols derived from Sub-Saharan African biomass fuels in smoldering fires

Markie'Sha James[a], Vaios Moschos[b,c], Megan M. McRee[b], Marc N. Fiddler[d], Barbara J. Turpin[c] , Jason D. Surratt[c,e], Solomon Bililign[a,b2 †]

[a] Department of Applied Sciences and Technology, North Carolina A&T State University, Greensboro, NC, USA

[b] Department of Physics, North Carolina A&T State University, Greensboro, NC, USA

[c] Department of Environmental Sciences & Engineering, University of North Carolina at Chapel Hill, USA

[d] Department of Chemistry, North Carolina A&T State University, Greensboro, NC, USA

[e] Department of Chemistry, University of North Carolina at Chapel Hill, USA

[†]Corresponding Author: Solomon Bililign; bililign@ncat.edu

The SI includes: 6 figures, and 4 tables

Number of pages: 12

Comment [BT]: Will the reader wonder why the peak aerosol mass concentration from the ACSM is so different from the peak from the SMPS?

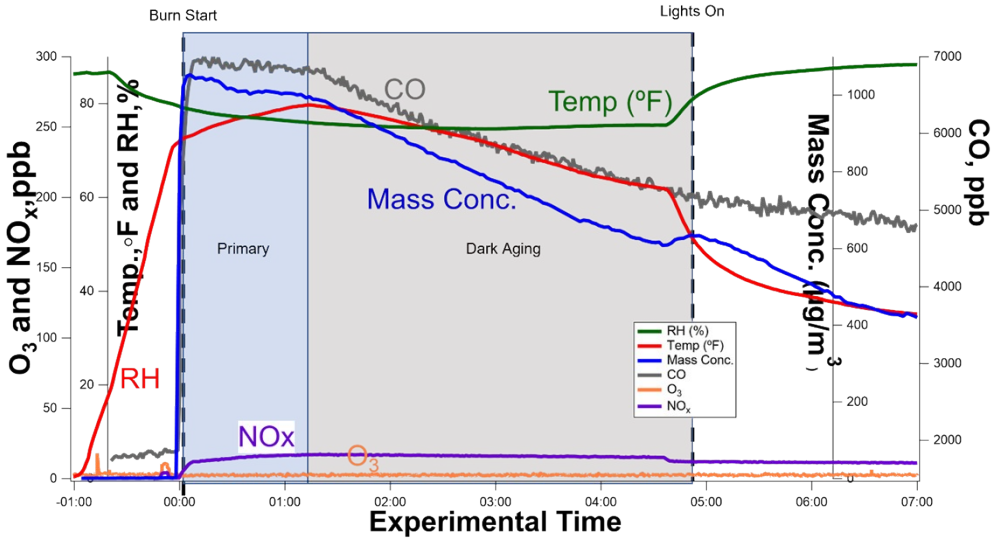

Figure S1. Time series of environmental and chemical parameters during a chamber experiment involving a humidified chamber (RH (≥65%). Mopane leaves were combusted and represented here. Y-axes report trace species concentrations (gases and particles), while the x-axis indicates experimental time. The graph displays RH (%), temperature (Temp, °F), aerosol mass concentration (Mass Conc, µg/m³), carbon monoxide (CO, ppb), ozone (O_3, ppb), and nitrogen oxides (NO_x, ppb) over time. The start of combustion, primary, dark aging, and photo-aging initiated by the UV lights are marked. Figure adapted from Mouton et al.[56]

Table S1. Detailed summary of the chamber experiments. The table includes the relative humidity (RH, %) inside the smog chamber at the start of combustion, calculated modified combustion efficiency (MCE), fuel mass burned (g), and whether the addition of the dark oxidant (NO_3•) was used during that particular experiment (burn). All fuels were combusted at 450 °C via a tube furnace. Due to gas analyzer and ACSM malfunctions, the blank indicates some values are unavailable.

Burn #	Fuel	RH	MCE	Mass Burned (g)	Peak Aerosol	Peak Aerosol	Addition of

					Mass Conc.	Mass Conc.	Oxidant
					(from ACSM)	(from SMPS)	
1	Mokala (*Acacia erioloba*)	<10 %	0.77	0.4865	---	633.8	---
2	Mokala (*Acacia erioloba*)	≥65%	0.75	0.0914	---	300.2	---
3	Mukusi (*Baikiaea plurijuga*)	≥65%	0.85	0.1692	45.5	651.2	---
4	Mopane Leaves (*Colophospermum mopane)*	≥65%	0.91	0.1639	71.8	529.9	---
5	Mopane Leaves (*Colophospermum mopane)*	<10 %	0.87	0.1590	32.8	335.3	---
6	Savannah Grass (*unknown*)	≥65%	0.88	0.1465	26.3	242.7	---
7	Mukusi (*Baikiaea plurijuga*)	<10 %	0.90	0.2588	43.8	587.9	---
8	Mopane Leaves (*Colophospermum mopane)*	≥65%	0.83	0.3107	413.9	885.7	Yes
9	Dung	≥65%	0.88	0.3830		917.2	Yes
10	Savannah Grass (*unknown*)	<10 %	0.82	0.4450	151.5	329.9	---
11	Mopane Leaves (*Colophospermum mopane)*	≥65%	0.83	0.4338	752.5	862.9	---
12	Mukusi (*Baikiaea plurijuga*)	≥65%	0.83	0.4148	149.0	718.6	---
13	Mukusi (*Baikiaea plurijuga*)	≥65%	0.74	0.4253	230.3	1240.0	Yes
14	Savannah Grass (*unknown*)	≥65%	0.93	0.4929	17.8	93.5	Yes
15	Mopane Leaves (*Colophospermum mopane)*	≥65%	0.87	0.5146	414.5	2010.0	Yes
16	Mokala (Acacia erioloba)	≥65%	0.79	0.3914	180.7	1460.0	Yes
17	Dung	<10 %	0.86	0.3761	229.1	870.5	---
18	Mokala (*Acacia erioloba*)	≥65%	0.79	0.3886	157.8	1303.0	---
19	Dung	≥65%		0.4257	744.5	509.7	---

Table S2. The results of statistical analysis are reported here, where z-score and two-sample t-tests, (95% CI, α:0.05) were used to determine if there was statistical significance of varying the mass of combusted fuel on the resulting mass spectra of the same fuel. Normalized data (f) values were used spanning across m/z 15-149. A Python code was written to read Excel files that contained f values; t-statistic and p-values are presented along with the results to accept the null hypothesis (H_0: $\mu 1 = \mu 2$).

Fuel	t-statistic (absolute value)	p-value	Result

Mokala	1.1997239958938792e-15	0.9999999999999991	Fail to reject the null hypothesis. There is no significant difference.
Mukusi	6.442303898093081e-16	0.9999999999999996	Fail to reject the null hypothesis. There is no significant difference
Mophane Leaves	1.4880290765174333e-15	0.9999999999999989	Fail to reject the null hypothesis. There is no significant difference
Savannah Grass	0.0011938676544102393	0.9990482413191994	Fail to reject the null hypothesis. There is no significant difference

Table S3. Detailed summary of the experiments used in PMF Analysis. The table includes the fuel, relative humidity (RH, %), aging condition data set included, and whether the addition of the dark oxidant ($NO_3^{\bullet}$) was used during that particular experiment (burn). All fuels were combusted at 450 °C via a tube furnace. Some experiments do not have the addition of oxidants are indicated by the dashed line. Those experiments only include dark and photoaging; upon exposure to oxidants combusted aerosols begin to age.

Burn #	Fuel	RH	Aging	Addition of Oxidant
1	Mopane Leaves (*Colophospermum mopane)*	<10 %	Primary Dark Photo	---
2	Savanna Grass (*unknown*)	≥65%	Primary Dark Photo	---
3	Mukusi (*Baikiaea plurijuga*)	<10 %	Primary Dark Photo	---
4	Savanna Grass (*unknown*)	<10 %	Primary Dark Photo	---
5	Mopane Leaves (*Colophospermum mopane)*	≥65%	Primary Dark Photo	---
6	Mukusi (*Baikiaea plurijuga*)	≥65%	Primary Dark Photo	---
7	Mukusi (*Baikiaea plurijuga*)	≥65%	Dark Photo	Yes
8	Savanna Grass (*unknown*)	≥65%	Dark Photo	Yes
9	Mopane Leaves (*Colophospermum mopane)*	≥65%	Dark Photo	Yes
10	Mokala (Acacia erioloba) Oxidation	≥65%	Dark Photo	Yes
11	Mokala (*Acacia erioloba*)	≥65%	Primary Dark Photo	---
12	Dung	≥65%	Primary Dark Photo	---

Table S4. Summary of fuels combusted in this study, including common names, scientific names, and fuel moisture content.

Common Fuel Name	Scientific Name	Fuel Moisture (%)
Mokala	Acacia erioloba	4.0±1.2
Mukusi	Baikiaea plurijuga	3.4±0.7
Mopane Leaves	Colophospermum mopane	7.8±.3
Savannah Grass	Unknown	<10
Cow Dung	N/A	<10

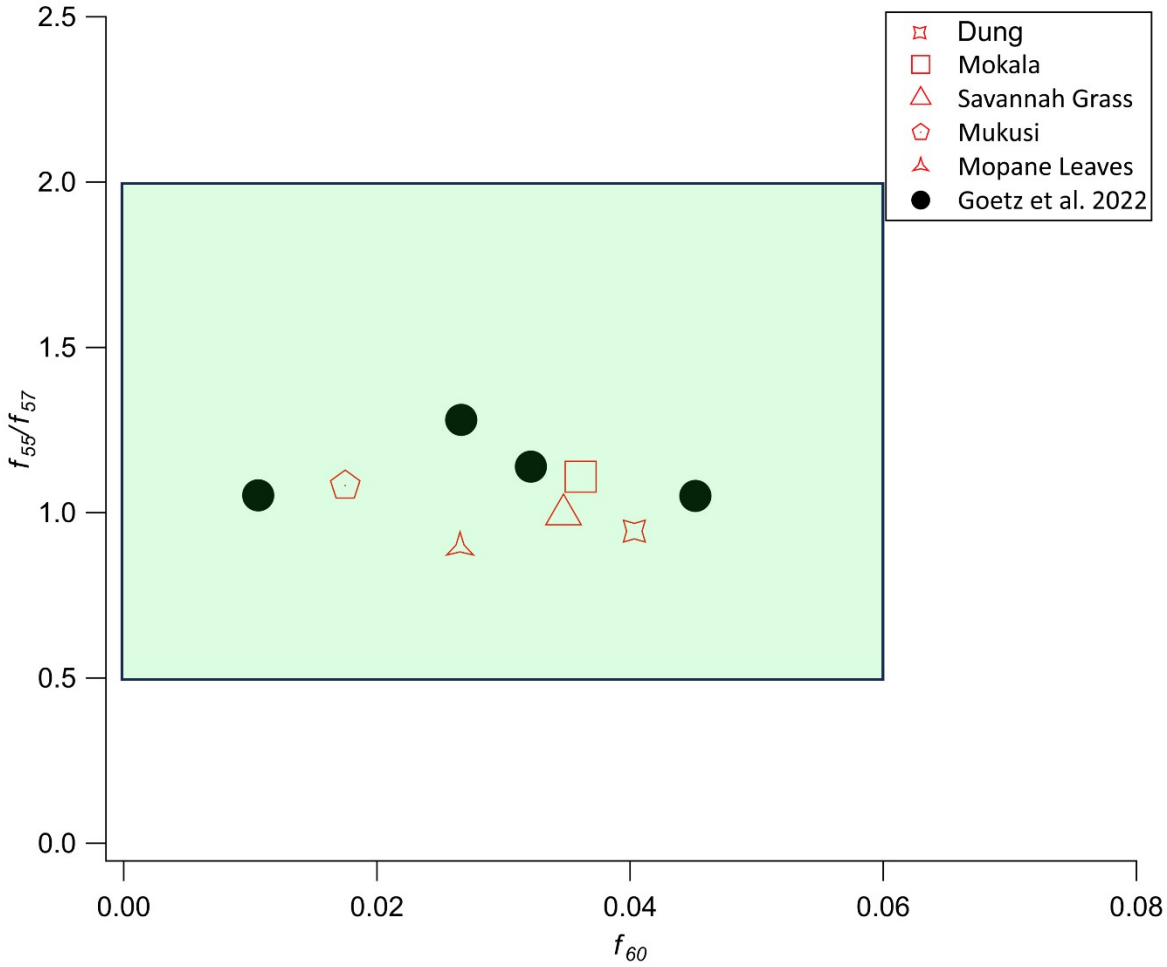

Figure S2. The f_{55} to f_{57} vs f_{60} average for each fuel source type. The green-shaded region includes the range of *f*-values for biomass burning profiles (including cookstoves and agricultural burns; the burn condition was not defined as smoldering or flaming dominant) reported by Goetz et al.[3] Literature values were extracted using WebPlotDigitizer. Labeled fuel sources report the average for the respective fuel type, including black dots for each respective fuel presented in Goetz at al.[3] and red open symbols for our experimental data.

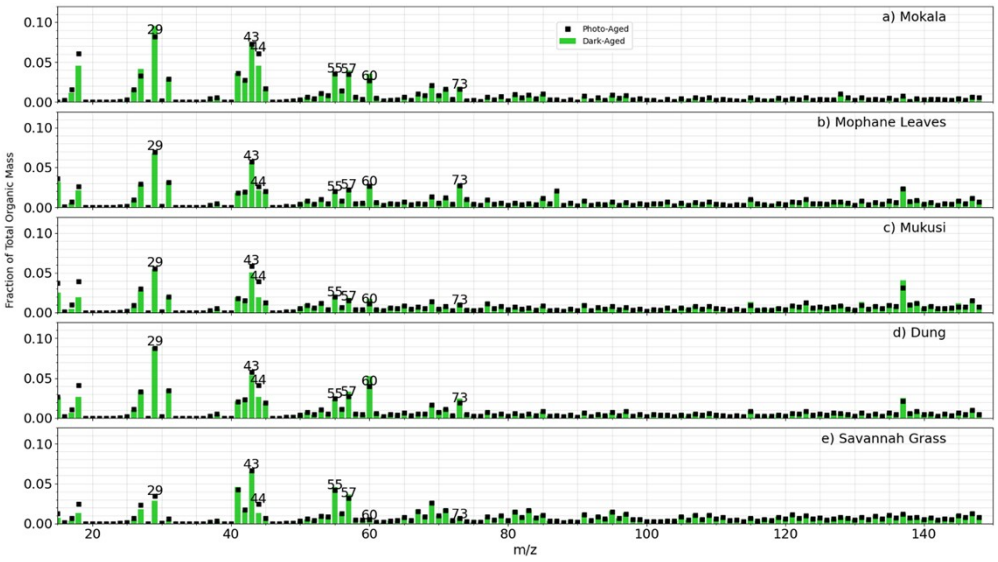

Figure S3. Mass spectra of the OA mass of fuels under dark- and photo-aged conditions in a humidified chamber (RH ≥ 65%). Note that dark aging (without $NO_3^{\bullet}$ present) was immediately followed by photoaging. The data presented is representative of mass spectra averaged over ~30 min within dark aging and photoaging.

Comment [BT]: At least the y-axis title and legend should have bigger fonts.

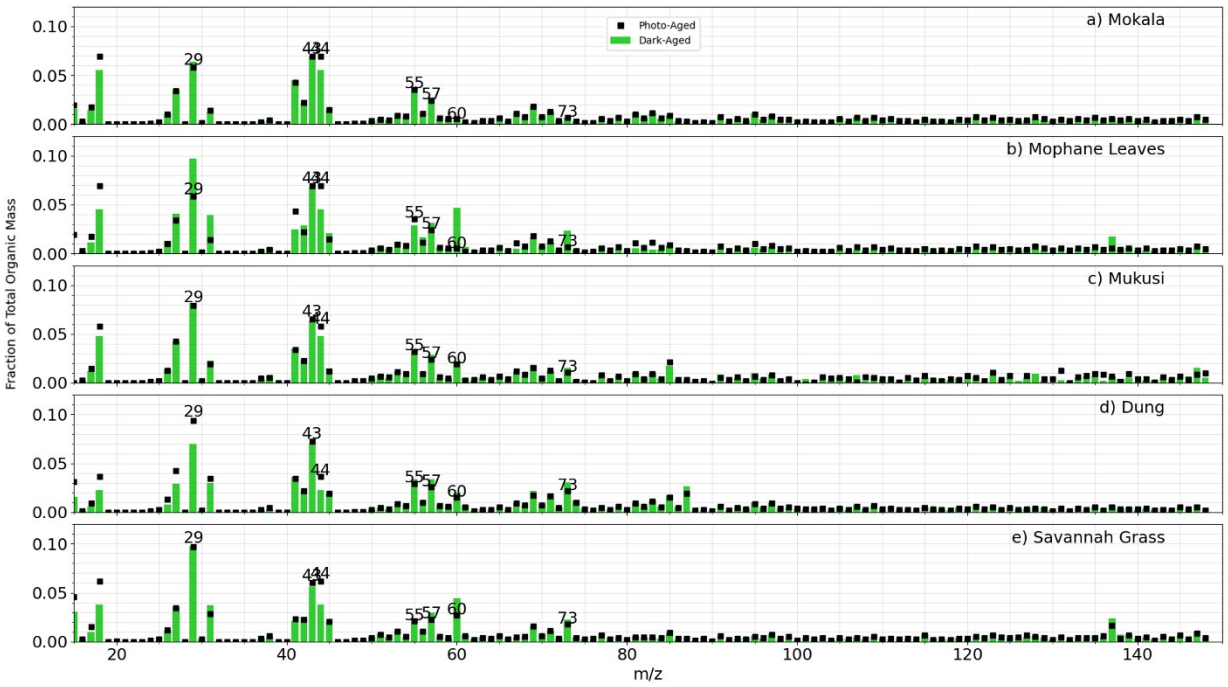

Figure S4. Mass spectra of experiments involving the addition of $NO_3^{\bullet}$; aerosols undergo 3 h of dark aging and 2 h of photoaging. Overall, mass spectra show increased oxidation in relevant *m/z* (f_{29}), 43 (f_{43}), 44 (f_{44}), 57 (f_{57}), 60 (f_{60}), and 73 (f_{73}).

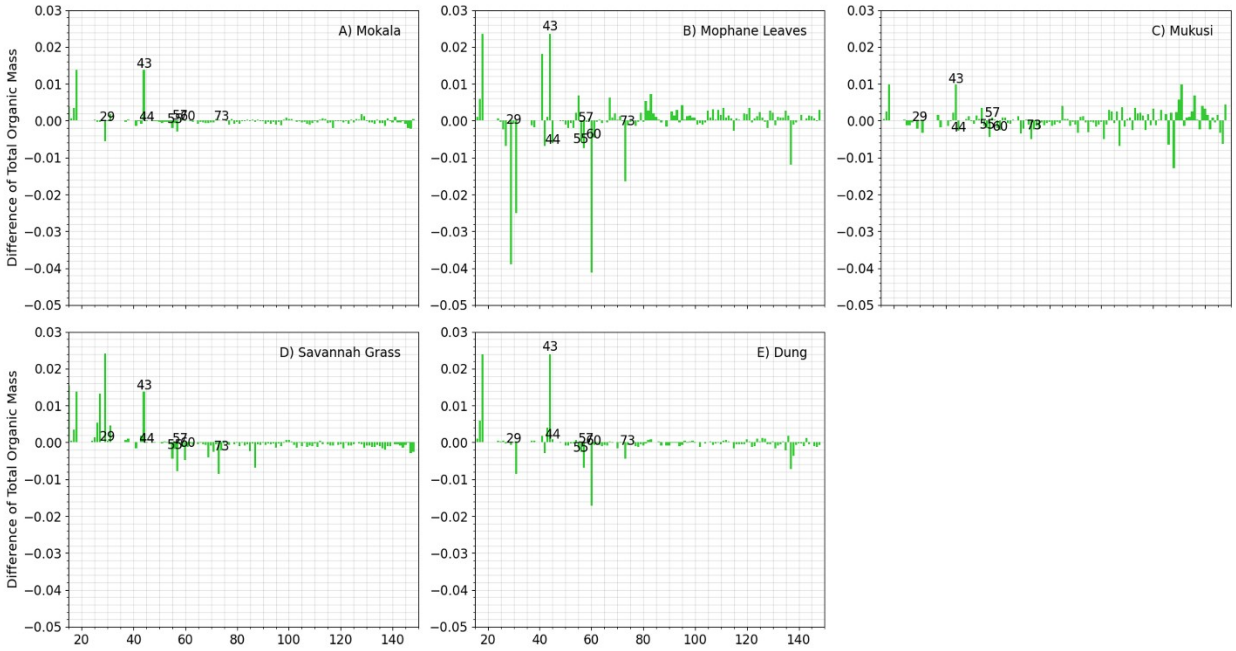

Figure S5. Time series of environmental and chemical parameters during a chamber experiment involving dark oxidation with NO_3 radicals in a humid chamber. Mopane leaves were combusted in the experiment shown. Y-axes report trace species concentrations (gases and particles), while the x-axis indicates experimental time. The graph displays RH (%), temperature (Temp, °F), aerosol mass concentration (Mass Conc, µg/m³), carbon monoxide (CO, ppb), ozone (O_3, ppb), and nitrogen oxides (NO_x, ppb) over time. The start of NO_3 radical generation, then injection of combustion emissions, followed by dark oxidation, and then dark aging, and photo-aging initiated by the UV lights are also marked (Figure adapted from Mouton et al.[61]).

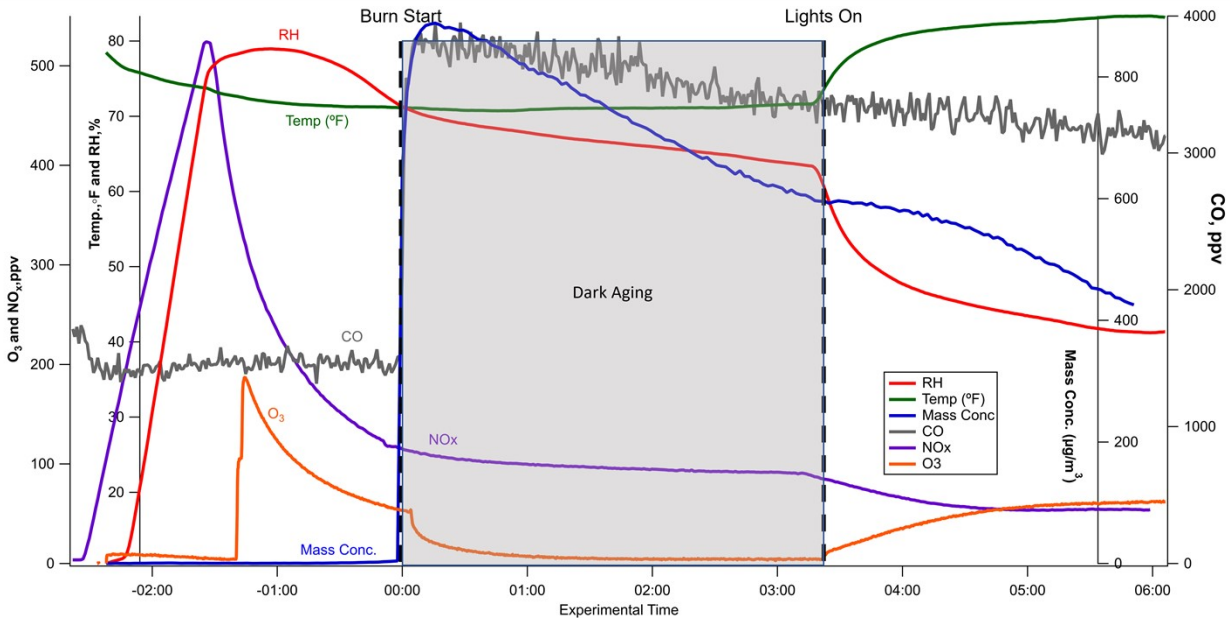

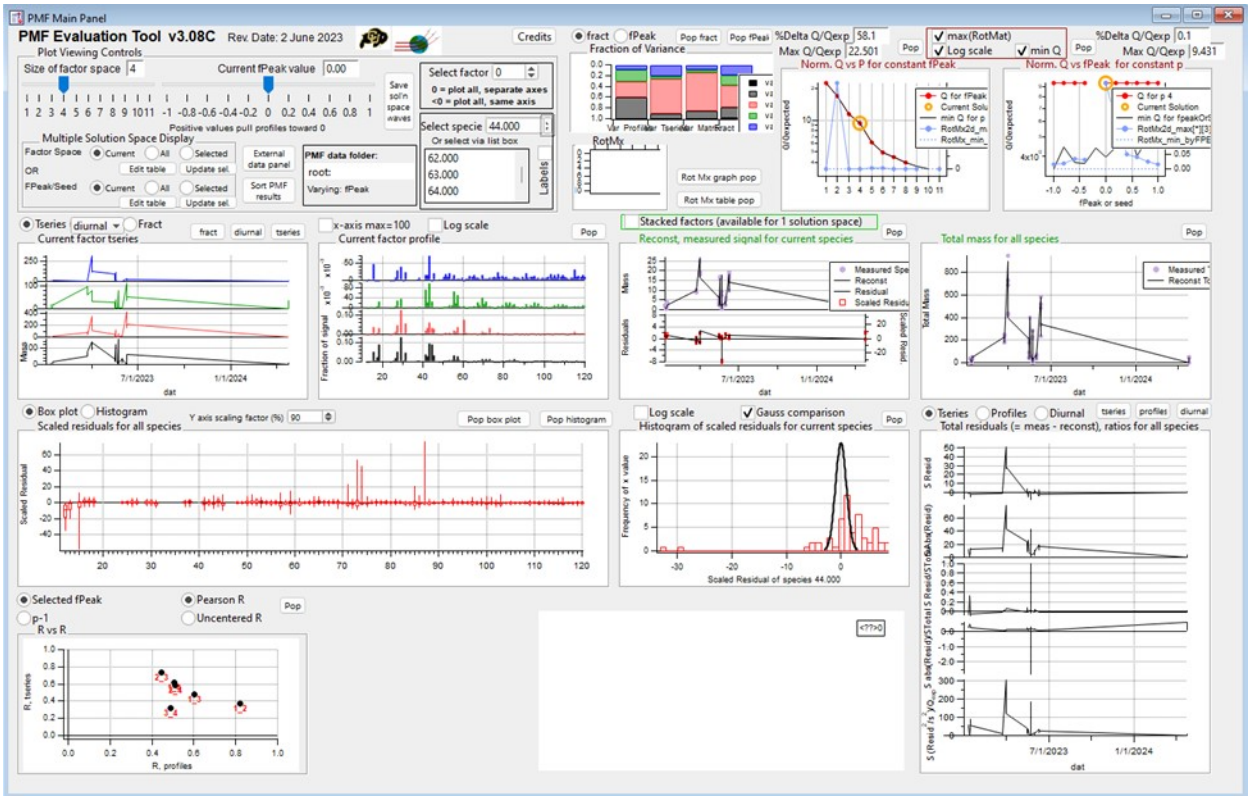

Figure S6. Screenshot of PMF Evaluation tool displaying the chosen factor solution, with panels representative of a 4-factor solution, representative of data used. PMF analysis comprised 12 data sets encompassing various aging and experimental conditions: fresh-, dark-, and photo-aging under both dry and elevated RH, as well as elevated RH with the addition of $NO_3^{\bullet}$ conditions. Time series and organic and organic error matrices data points from within each aging condition were chosen as follows: 1 fresh data point, 2 dark aged data points, consecutive, and 2 photo-aged data points. Data points are from the last 1 or 2 15-minute time intervals from within the 1-hour (fresh), 3-hour (dark-aging), and 2-hour (photo-aging) before analysis.

Details of PMF Analysis of OA Mass Spectra:

A run with a factor space size of 2-11 and min/max seed *FPEAK* of 1.0 and 20, respectively, and Δ *FPEAK* =2.0, was chosen to determine the number of sources. *FPEAK* is a rotational parameter that can be adjusted to explore the stability and interpretability of factor solutions; with an *FPEAK* =2.0 the factor profiles demonstrated clearer distinctions between contributing sources. Ideally, the model would have a Q/Q_{exp}=1.0;[74] however, Ulbrich et al.[69] determined this criterion alone is not sufficient for choosing the best number of factors to determine an acceptable solution. The final solution reports a Q/Q_{exp} value of 22.5 and f peak value of 0. This value is not comparable to other studies where AMS or ACSM data was used for PMF, where Q/Q_{exp}<10.[101 48, 50, 89, 95] Solutions between data sets were compared following methods mentioned in Section 2.8. A significant change in Q/Q_{exp} was observed for solutions 1-3 before tapering off at solutions 4-11. Residuals for *m/z* 15-120 reported a

Gaussian shape. Exploration of each solution was done, with 4 solutions showing the minimal number that allowed the identification of sources. Solutions 5-11 presented replicates of factors, proving negligible solutions.

A 4-factor solution was chosen to deconvolve OA mass spectra produced via the ACSM. This solution provides enough factors to resolve the lowest-abundance components; increasing the number of factors past 4 led to increasing factor splitting without providing additional insight. Factors for the 4-factor solution are described in results, below.

Comment [BT]: I would move all of this to methods. If not, then put it in SI and tell the reader about it in methods.

Reference List

1. R. P. Pokhrel, J. Gordon, M. N. Fiddler and S. Bililign, Impact of combustion conditions on physical and morphological properties of biomass burning aerosol, *Aerosol Science and Technology*, 2021, **55**, 80-91.
2. D. M. Smith, M. N. Fiddler, K. G. Sexton and S. Bililign, Construction and Characterization of an Indoor Smog Chamber for Measuring the Optical and Physicochemical Properties of Aging Biomass Burning Aerosols, *Aerosol and Air Quality Research*, 2019, **19**, 467-483.
3. J. D. Goetz, M. R. Giordano, C. E. Stockwell, P. V. Bhave, P. S. Puppala, A. K. Panday, T. Jayarathne, E. A. Stone, R. J. Yokelson and P. F. Decarlo, Aerosol Mass Spectral Profiles from NAMaSTE Field-Sampled South Asian Combustion Sources, *ACS Earth and Space Chemistry*, 2022, **6**, 2619-2631.